Chapter 5

The giant impact or a model for Moon formation

5.1 The formation of the Moon

Despite its relatively close proximity compared to other astronomical objects, the formation of the Earths Moon presented a mystery deep within the space-age. In the 1960ies, sample-return missions like Apollo or Luna brought geological insight into the Moon. While not directly shedding light on the formation itself, these lunar samples showed that the Earth and the Moon have an identical signature in oxygen isotopes down to measuring uncertainty, opposing the heterogeneity in isotopic signatures in the solar system (Wiechert et al. 2001). This suggests, that the Moon has formed from the same material as the Earth. Another constraint on a formation theory of the Moon, is a relative depletion in iron. Seismic measurements on the Moon and also its bulk density suggest, that the Moon has an iron core with lass than 5% of its overall mass (Weber et al. 2011). Another dynamical constraint on a theory for lunar formation is the conservation of the Earth-Moon systems angular momentum since its formation within 10% of its initial value (Canup et al. 2001).

Until the mid 1970ies, only three formation models have been known, all of them with their shortcomings (Stevenson 1987). The fission theory goes back to the 19th century and proposes, that the Earth gained angular momentum due to some unknown mechanism and the rotation period went below the limit for rotational stability ($< 2.1h$). Part of the Earth was then shed into Earth orbit and re-accumulated into a satellite, which became our Moon. While this theory matches nicely the composition constraints, this formation mechanism would leave the Earth-Moon system with an angular momentum three times higher than todays value. Another theory suggests, that the Moon is simply a body which formed elsewhere and was later on captured into an

orbit around the Earth. Aside from it's dynamical implausibility, it fails to explain the Moons iron depletion. A third theory proposes the co-accretion of the Moon in parallel to the Earth. While similar models might work well for the Giant planets moons, it fails to explain the relatively high angular momentum of the Earth-Moon system.

5.2 The giant impact theory: Review of past work

A more promising approach was the *giant impact* theory first proposed by Hartmann and Davis (1975) and Cameron and Ward (1976). They suggested, that todays Moon is a left-over of a giant impact between the forming Earth and an impacting second largest body from the proto-Earth's vicinity. The impact leaves debris in an Earth orbit, which later on accretes into the Moon. This model not only explains the high angular momentum of the Earth-Moon system, but also permits impact processes to account for the iron depletion of the Moon.

While Hartmann and Davis (1975) put the impactor size on a rather small $R \approx 1200km$ ($\approx 0.0048M_{\oplus}$ for a density of $4g/cm^3$) based on a simple energy budget, Cameron and Ward (1976) advocated for a larger body in the Mars mass regime ($\approx 0.1M_{\oplus}$). Despite those estimates, the model remained qualitative and lacked quantitative verification. It was not until 9 years later, when the theory spur major interest at the *Origin of the Moon* Kona conference in 1984. The advancement in numerical techniques, most notably SPH, and the now available computing power meant, that the theory could be put a for a test.

In terms of time scales, the giant impact theory can be split up into three distinctive phases: The first phase is the actual impact. This happens on the order of the collisional timescale (see section 3.1) which yields $\approx 24h$ in case of the proto-Earth. Debris is put in orbit around the Earth. During a second phase, this debris accretes into individual moonlets, a process happening on $50 - 1000\tau_K$ [1] corresponding to a few months. In a third and final phase, these moonlets then undergo orbital evolution over millions of years due to tidal interaction with the proto-Earth and under circumstances even might collide if there were more than one Canup and Esposito (1996).

The first direct simulations (Benz et al. 1985, 1989; Cameron 2000) of the actual impact not only showed that the basic mechanism of the giant impact actually work, but also delivered first quantitative estimates on the required impact parameters for successfully putting enough material into Earth orbit. Already Hartmann and Davis (1975) noted that about two lunar masses ($2M_{\leftmoon} = 0.024M_{\oplus}$) of silicates in orbit around the proto-Earth are required to later on successfully form the Moon. Similar results were obtained by N-body simulations of the accretion phase of the giant

[1] τ_K denotes the Kepler time at the Roche limit for lunar density material of the proto-Earth ($\approx 2.9R_{\oplus}$) and yields $\approx 7h$

impact theory: Canup and Esposito (1996) found that either a bit more than a lunar mass outside the Roche limit or more than two lunar masses near or inside the Roche limit are sufficient for lunar accretion. Additionally they found that when most of the disk mass lies outside the Roche limit after the impact, multiple moonlet formation occurs. In this case tidal torques will change the orbit of the heavier moonlets more rapidly. So if the moonlet mass decreases with distance from the proto-Earth, the heavier moonlets will migrate outwards faster and outrun the lighter moonlets, ultimately colliding with them and forming one large Moon. Ida et al. (1997) performed a similar study and found scaling laws for the final moon mass in as a function of the mass and angular momentum of the proto-lunar disk. They showed, that the disk material can accrete into a Moon with an efficiency of $15\% \ldots 40\%$, depending on the mass distribution and the angular momentum in the disk. Similar work by Kokubo et al. (2000) included a better collision handling in their N-body code and found similar results. The scaling laws from both studies agree well with the early results from Canup and Esposito (1996) and show that disk masses of $\approx 1.5 \ldots 2.0 M_{\leftmoon}$ are required to successfully accrete a Moon mass satellite.

The conundrum giant impact simulations have to solve is to find suitable impact parameters, leading to the desired post-impact configuration of the disk. Giant impact simulations require at certain resolution, in order to resolve the proto-lunar disk sufficiently. As collisions of bodies lack any inherent symmetry, such simulations have to be undertaken in 3D. For grid-based schemes resolution is defined spatially. This means that the hydrodynamics at the time of impact need to be sufficiently well resolved while still covering the entire proto-lunar disk after the impact. For a Lagrangian code like SPH, the resolution is given by the smallest mass element. With the proto-lunar disk containing only a few percent of the Earth-Moon systems total mass, a number of at least a few thousand particles is required in order to resolve the disk sufficiently.

The parameter space for the impact is comparable to the study performed in chapter 3 of this thesis, with the four major parameters being target mass, mass ratio, impact angle and velocity: $\{M_{targ}, \gamma, \theta_{imp}, v_{imp}\}$. Other parameters like composition of the colliding bodies were never considered to be free. Practically all simulations assumed, that both the target and the impactor are differentiated and of chondritic composition ($70wt\%$ silicates and $30wt\%$ iron core). In the 1980ies, parameter studies with an extent comparable to the one in chapter 3, compromised of several thousand simulations each using thousands of particles, were simply not feasible due to limitations in computing power. Early work (Benz et al. 1985, 1989; Cameron 2000) thus tried to constrain the parameter space as much as possible by certain assumptions and then only performed a handful of simulations located in the corresponding parameter subspace.

A very strong constraint on the parameters is given by assuming mass conservation during the impact thus $M_{imp} + M_{targ} \approx M_{lr}$, where M_{lr} is the mass of the largest remnant or in the particular case of the giant impact the Earth-Moon system. Depending on the timing of the gi-

ant impact during the proto-Earths accretion, the total mass is either chosen to be a fraction of or the whole mass of the Earth-Moon system $M_\oplus + M_\leftmoon \approx M_\oplus$. For a given largest remnant mass, the mass conservation assumption thus gets rid of one free parameter. With mass conservation, also the angular momentum is conserved, so that $L_{imp} \approx 1.1 - 1.2 L_{\text{E-M}}$ (Canup et al. 2001). Note that this assumption is weaker, as even a small mass loss can lead to a considerable loss of angular momentum. The mass ratio is then constrained by the maximum angular momentum an impact can deliver at $\theta_{imp} = 90°$ (or $b = 1$) where $L_{\text{imp}} = L_{\text{graz}}$. This puts a lower limit of $\gamma > 0.08 \ldots 0.09$ (Canup and Asphaug 2001). Under the assumption of mass conservation, the impact angle is for a given mass also determined by the angular momentum, as $L_{\text{imp}} = L_{\text{graz}}(M_{targ}, M_{imp}, v_{imp}) \sin\theta_{imp} \approx 1.1 - 1.2 L_{\text{E-M}}$. Thus the number of free parameters reduces to two. The impact velocity is also somewhat constrained, as high impact velocities lead to mass loss and would violate the initial assumption.

Benz et al. (1989) used for the impact velocity values of $v_{imp} = v_{esc}$ ($v_{-\infty} = 0$), but interestingly also tried out scenarios with $v_{imp} \approx 1.4 v_{esc}$ ($v_{-\infty} = 10 km/s$). They found that slow collisions ($v_{imp} = v_{esc}$) with an impactor mass of $M_{imp} = 0.11 \ldots 0.14 M_\oplus$ and a total mass of $M_{targ} + M_{imp} = 1 M_\oplus$ to be able to produce massive enough and iron-depleted proto-lunar disks. While the high velocity collisions also produced considerable disk masses, they were rejected because of a too large iron content (up to $1.3 M_\leftmoon$). It is important to note that this simulations used only 3008 particles and therefore resolved the disk with only $60 \ldots 100$ particles! Determining the iron content of such a disk goes beyond the resolution. The iron percentage upper limit corresponds to only 5 iron particles and anything above that will be considered an iron excess. After this finding for high velocity collisions, later work never considered collisions with $v_{imp} > 1.10 v_{esc}$ again.

Simulations by Cameron (1997) with considerably higher resolution had trouble reproducing the initial results by the series of papers by Benz. He found the optimum range for the mass ratio to be $\gamma = 0.25 \ldots 1.0$ and the total mass of $M_{tot} = 1 M_\oplus$ in order to put enough material into orbit, but only with a rather high $L_{\text{imp}} \approx 2 L_{\text{E-M}}$. Thus he put forward an *early scenario* in which the impact occurs when the Earth has accreted only part of its mass, so that $M_{targ} \approx 0.5 M_\oplus$. In Cameron (2000) he showed with $10k \ldots 100k$-particles simulations, that a collision with $\{0.45 M_\oplus, 7 : 3, 1.00 v_{esc}\}$ and a suitable impact angle to yield $L_{imp} \approx 1.1 L_{\text{E-M}}$ to be successful in putting roughly two lunar masses into orbit with the right amount of final angular momentum. He also found the escaping mass to increase for slight increases of the impact velocity and used this as an argument for not considering further simulations with higher impact velocities. The main problem with this *early impact* scenario remained that the Earth-Moon system still has to accrete $\approx 0.35 M_\oplus$ until its final configuration. It is unlikely that the Moon would have kept its iron depletion during this post-impact accretion period.

Canup et al. (2001) still followed the path of the *late impact* scenario and confirmed with $10k \ldots 100k$-particles simulations the same issue found by Cameron (2000): Late impacts only produce massive enough disks, when an excess angular momentum of $L_{\text{imp}} \approx 2L_{\text{E-M}}$ is used. But their conclusion was different. As one possible explanation, Canup et al. (2001) state: *If we assume that the Moon did in fact form via a large impact event, this finding suggest one or more of the following: (...) (2) regions of parameter space not explored in the above surveys could suggest different scaling relationships that would more easily yield the Earth-Moon system (...).* Although Canup and Asphaug (2001) were also unable to produce disks masses above $2M_{\leftmoon}$, they found that the satellite mass scaling law from (Kokubo et al. 2000) yields satellite masses above a Moons mass for impacts with $\{0.88M_{\oplus}, 0.1, \approx 53^{\circ}, 1.00v_{esc}\}$. So far, this has been considered to be the most promising impact scenario for the giant impact. We call it the *canonical model.*

Later work (Canup 2004) concentrated on finding scaling laws for the disk mass in the low velocity regime. Similar to the early work by Benz et al. (1989), they found that grazing collisions tend to produce iron-rich disks for $v_{imp} > 1.1v_{esc}$ and thus also rejected the possibility of a high velocity impact. More recent work (Canup 2008) extended the parameter space by considering pre-impact rotation of both the target and the impactor. Interestingly, high velocity impacts up to $v_{imp} = 1.4v_{esc}$ were investigated, although still with the same basic assumption of no mass escape. For that reason, these high velocity collisions were still performed with $L_{\text{imp}} \approx 1.1L_{\text{E-M}}$, although the final angular momentum is lower with mass loss. Disk masses were found to be well below the required values for moon formation. The overall conclusion of this work was, that target pre-impact rotation might be favorable for Moon formation.

Impact simulations with other methods than SPH are sparse: The first simulations with a grid code incorporating hydrodynamics and self-gravity, were performed by Wada et al. (2006). They performed a few simulations in the low-velocity regime comparable to previous SPH work. These grid code results agreed in general with the SPH results, despite only using very simple polytropic equations of state. This is very not surprising, as the collisions occur in the gravity regime and are largely dominated by gravitational processes. More recent work (Canup and Barr 2010) compared simulations performed with the Eulerian CTH code with the SPH results and also found the basic results to agree during the first few hours of the impact.

The main problem of the canonical model is the disagreement with the geo-chemical evidence: The canonical model predicts, that $70 \ldots 80\%$ from the disk material originates in the impactor. The isotopic similarity in oxygen isotopes between the Earth and the Moon thus heavily contradicts the observed heterogeneity in the solar system (Wiechert et al. 2001). A model has been put forward (Pahlevan and Stevenson 2007; Pahlevan et al. 2011) which explains the isotopic similarity by re-equilibration of the oxygen isotopes through thorough mixing in the presumably hot proto-lunar disk after the impact event. It is still a qualitative model and lacks validation through direct

simulations of the proto-lunar disk. A major problem of the model is the requirement, that all the silicate reservoirs mix with each other efficiently. Thermal inversion layers in the proto-Earth or clumps quickly being formed right after a accretion, a phenomenon often observed in simulations (Cameron 1997, 2000; Canup and Asphaug 2001; Canup 2004) would prevent efficient mixing and inhibit the individual reservoirs of oxygen to re-equilibrate.

5.3 Alternative impact scenario

The last section showed, that only a limited region of the parameter space for the giant impact has been studied so far. The fact that a successful model was found in the low velocity regime, does not exclude the possibility of other regions containing potential Moon-forming impacts. The search for new scenarios has been triggered for example by exotic models like Wolbeck and Connolly (2010), who suggest an *icy impactor model* and argue that the impactors energy from beyond the ice line would provide much more kinetic energy available for the impact. The gain in kinetic energy for an impactor migrating from the solar system snow line ($\approx 2.7AU$) to the Earths orbit leads to $v_{-\infty} = 33km/s$ or in case of a $\{0.9M_{\oplus}, 0.2\}$ impact to an impact velocity of $3.78v_{esc}$. Such collisions are mainly disruptive and unlikely to lead to the formation of a relatively massive satellite. Nevertheless, it is important to check such alternative scenarios for viability with direct simulations.

Figure 5.1 shows the largest remnants disk mass for the simulation set *c1* from the parameter study in chapter 3. Unlike the previous studies which only covered limited regios of the parameter space, this plot gives a complete overview of the parameter subspace for a given target mass and mass ratio. Although neither the target mass nor the mass ratio exactly match the values used in previous work and especially the canonical model by Canup and Asphaug (2001), the different velocity and impact angle regimes leading to considerable disk formation are recognizable. In case of $\{1M_{\oplus}, 0.1 \ldots 0.2\}$, a two lunar masses disk corresponds to $M_{disk}/M_{tot} \approx 0.03$. The low velocity regime with $v_{imp} = 1.00 \ldots 1.10$ can be clearly identified for grazing impact angles. Interestingly, for $\gamma \geq 0.2$ there exists a very narrow range of impact angles, for which also high velocity impact produce disks with a considerable mass. For example the largest remnant in $\{1M_{\oplus}, 0.1 \ldots 0.2, 1.30v_{esc}, 37.5°\}$ has a disk with a mass of $M_{disk} \approx 0.05M_{tot}$ after the collision. It was noted in the previous section, that Benz et al. (1989) already performed collisions in a similar velocity regime and also noticed disk formation. But they rejected the case due to relatively high amounts of iron in the disks.

The simulations from the parameter study in chapter 3 use a relatively small number of particles ($\approx 100k$). From looking at figure 5.1 it becomes apparent that the disk masses for the high

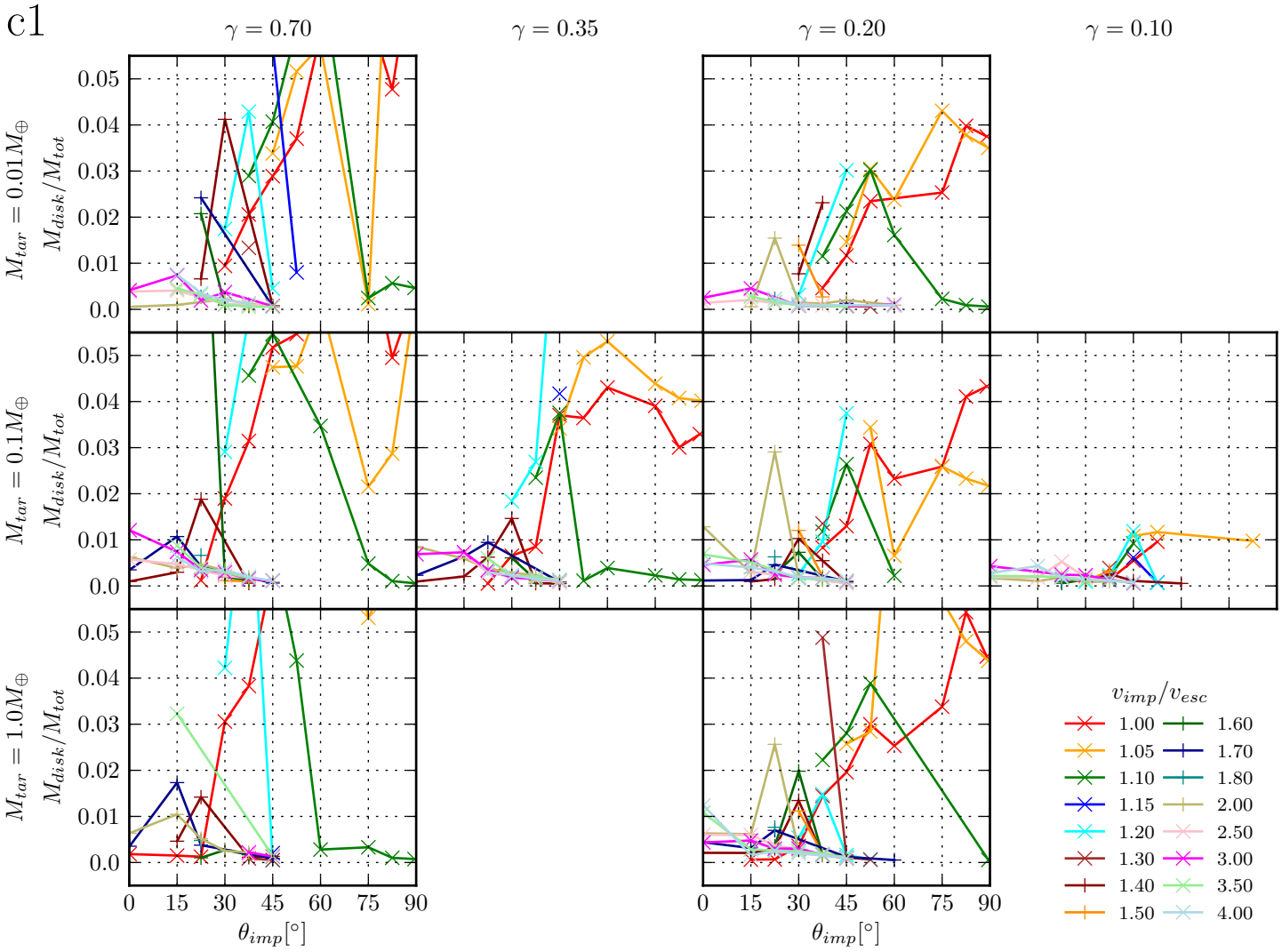

Figure 5.1: Largest remnant total disk mass as a function of impact angle for different impact velocities for the *c1* simulation set from the parameter study in chapter 3. Simulations with a largest remnant disk mass below $0.01\% M_{tot}$ are omitted.

velocity regime ($v_{imp} = 1.20 \ldots 2.00$) are less independent on the parameters than in the low velocity regime ($v_{imp} = 1.00 \ldots 1.10$). For $\gamma = 0.2$, the low velocity cases show considerable disk masses for a wide range of impact angles and also don't vary much between the individual target mass regimes. The high velocity regime is different: The $\{1M_{\oplus}, 0.1 \ldots 0.2, 1.30v_{esc}, 37.5°\}$ case with a relatively massive disk for example appears to be an isolated case as a function of impact angle and occurs only for $M_{targ} = 1.0M_{\oplus}$. These narrow ranges for efficient disk formation occurs for the entire high velocity regime.

Qualitatively this can be explained by the basic mechanism behind disk formation: In order for material to end up in orbit around the largest remnant central clump, it requires to have the right orbital energy. If it's too low, the material is accreted onto the clump, if it's too high it escapes the remnant. In the low velocity regime, the disk is mainly compromised of the impactor material. Its initial orbital energy is already near the upper limit for which material is gravitationally bound as $v_{imp} \approx v_{esc}$. Disk formation in this regime happens for relatively grazing angles, so most of the impactor material is only mildly decelerated and enters a bound orbit around the target or the later largest remnant. The required reduction in orbital energy is small compared to the range of orbital energy the material can have so that it ends up in the disk. The contrary applies in the high velocity regime: The required reduction of orbital energy is large compared to the required range. It's more difficult to hit the right amount of orbital energy, as the allowed range is easily missed. This change is also more dependent on the actual impact geometry, as these collision occur at smaller angles than in the low velocity regime.

In order to investigate the high velocity regime more thoroughly, we performed a set of high-resolution simulations with half a million particles. The details and the results are described in detail in the manuscript below, but the covered parameter space will be quickly discussed to put it into the context with the review of previous work. Figures 5.2 and 5.3 show a few of those simulations and their location in the parameter space. The individual points also show the key results which give the potential for successful formation of an iron-depleted Moon massed satellite: The mass of the silicates and the iron in the disk and the total angular momentum bound in the largest remnant. The color additionally give the target material depletion, which will be explained in the following manuscript.

As expected, for grazing collision ($\theta_{imp} = 45 \ldots 50°$) similar results are obtained as in the work previously mentioned. Relatively massive disks form with a fraction of the impactors mass. The disks are iron depleted and the resulting angular momentum corresponds roughly to the initial angular momentum of the collision. For $M_{imp} = 0.10M_{\oplus}$ (top plot, figure 5.2), the results in the low velocity regime correspond to the canonical model and fit the constraints for Moon formation, while for $M_{imp} = 0.20M_{\oplus}$ (bottom plot, figure 5.2) the angular momentum is too high due to the high impactor mass. Also shown in the plots are dashed lines for points in the

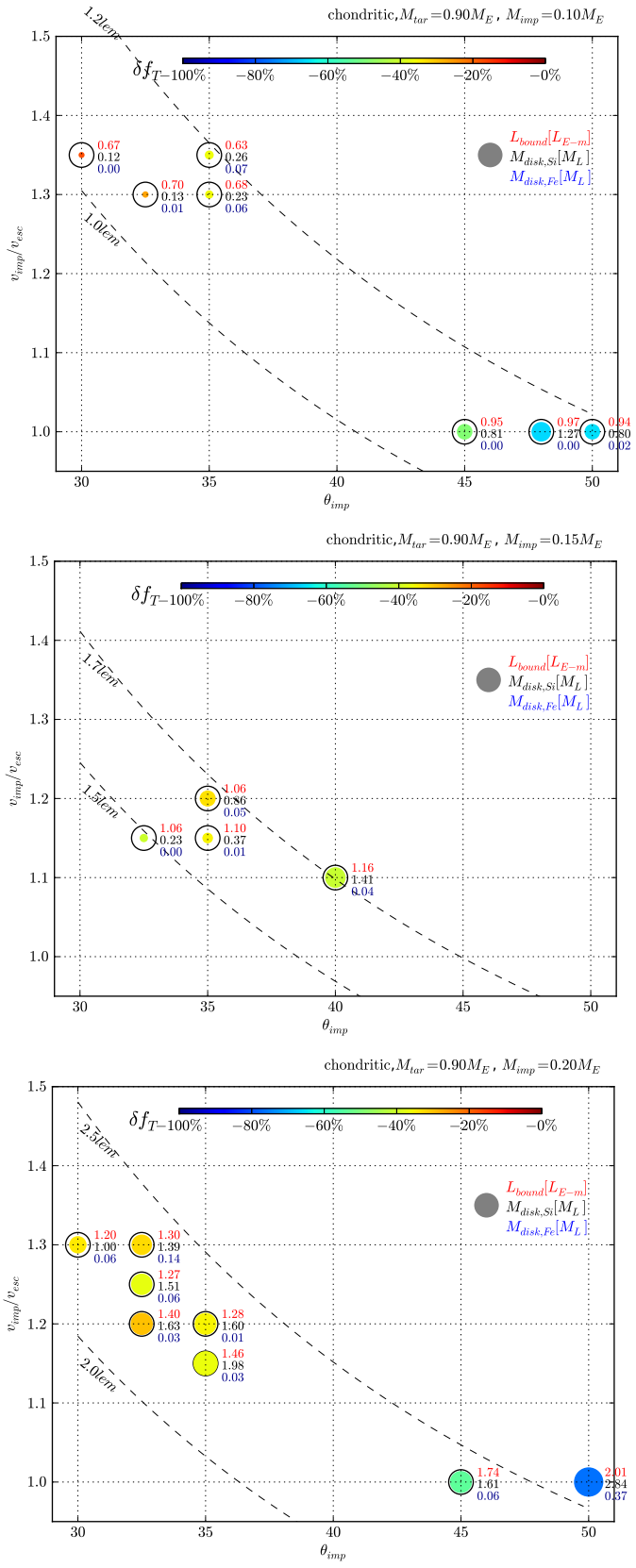

Figure 5.2: Parameter space view of the simulations with chondritic impactor composition, each panel shows a different impactor mass. Every simulation is shown as a filled circle with an area proportional to the silicate disk mass $M_{disk,\mathrm{SiO_2}}$. The black circle gives $2M_{☾}$ for reference. The color depicts the depletion factor in target material δf_T. Besides each circle, the bound angular momentum in $L_{\mathrm{E\text{-}M}}$-units, the silicate disk and the iron disk mass in Moon masses are further noted.

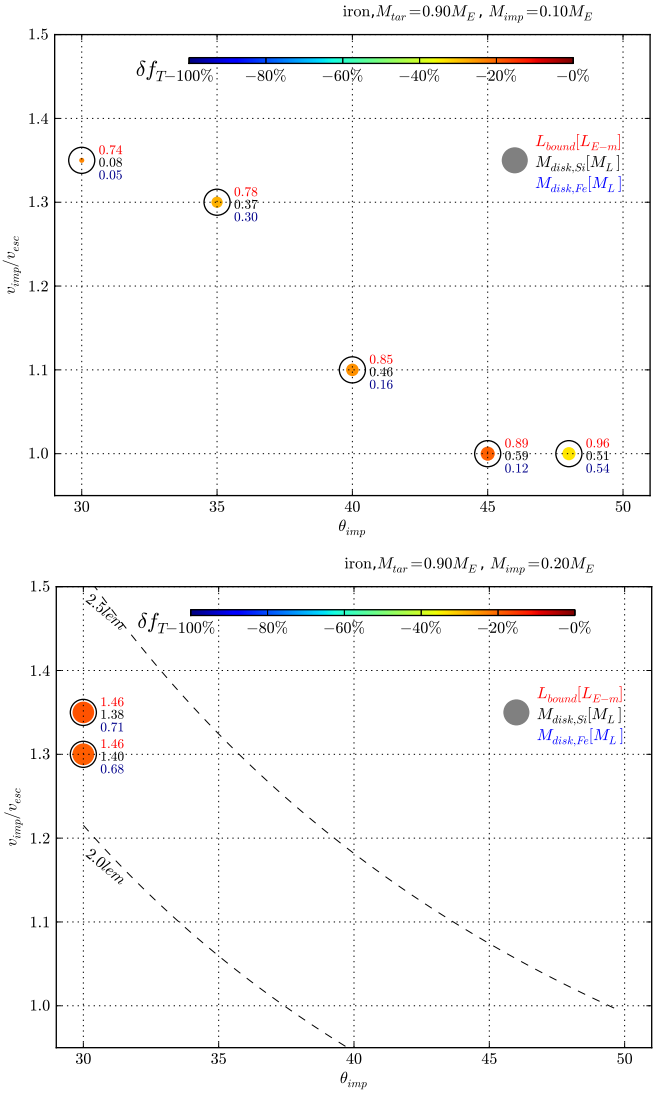

Figure 5.3: Same parameter space plots as in figure 5.2 but for the simulations with an iron impactor (70wt% Fe and 30wt% silicates.

impact parameter space with the same L_{imp}. When we now switch to the high velocity regime ($v_{imp} = 1.30 \ldots 1.35 v_{esc}$) the efficiency for disk formation is very low, resulting in disk masses roughly a magnitude too small for Moon formation. But another important effect is visible: The final angular momentum of the largest remnant is only about half of the initial amount due to mass loss during the collision. This means we can use a higher initial angular momentum. If we stay in the same region in terms of impact velocity and angle, we can increase the impactor mass. The trend becomes apparent for $M_{imp} = 0.15 M_{\oplus}$ (middle plot, figure 5.2), where for example $\{1.20 v_{esc}, 35°\}$ delivers already quite satisfying results, despite a slightly too small disk mass. The $\{1.10 v_{esc}, 40°\}$ case lies in between the low and high velocity regime and delivers a disk massive enough for Moon formation while also fulfilling the other requirements. When we raise the impactor mass to $M_{imp} = 0.20 M_{\oplus}$, the high velocity regime becomes interesting: While the disk mass in the low velocity regime is roughly proportional to the impactor mass, the disk mass increases more radically for the heavier impactor in the high velocity regime. For $v_{imp} = 1.15 \ldots 1.30 v_{esc}$ and $\theta_{imp} = 30 \ldots 35°$, there exists a set of collisions leading to relatively heavy, iron-depleted disks and a final angular momentum between $1.20 \ldots 1.40 L_{\text{E-M}}$. While in some cases the iron content or the angular momentum is too high, they reveal that this region of the parameter space can successfully deliver a post-impact situation suitable for Moon formation. By dropping the assumption of no mass loss, we have therefore found a new region in the parameter space with potentially Moon forming impacts.

The main difference in the initial conditions of these cases is the higher impact mass and impact velocity compared to the canonical case. Whether the canonical model or the high velocity cases presented here suit better the available models of terrestrial planet formation is a difficult question. With the giant impact being only one single event means that the question to be answered is which model is more probable. Chambers (2001) for example came to the conclusion, that the median mass to hit the proto-Earth is $0.22 M_{\oplus}$ with a median $\gamma = 0.67$. While this does not directly favor our model, it shows at least that such an impact would be compatible with this terrestrial planet formation model. More recent work by O'Brien et al. (2006) also suggest that such high velocity collisions are possible. Their median values for M_{imp} and $v_{-\infty}$ do not favor either of the two velocity regimes. The following manuscript will now discuss the results in detail and also discuss the current geochemical evidence in the light of these new results.

manuscript to be published

Making the Moon from the Earths mantle

Andreas Reufer, Matthias M. M. Meier, Willy Benz and Rainer Wieler

The formation of the moon from a disk formed by a collision between the proto-Earth and a roughly Mars-sized impactor is widely accepted today. This *giant impact* hypothesis (Cameron and Ward 1976) explains the high angular momentum of the Earth-Moon system and the moon's deficiency in iron. Hydrodynamical simulations have shown that a differentiated impactor with a chondritic Si/Fe ratio hitting the proto-Earth at mutual escape velocity and a grazing impact angle of 45° can lead to a proto-lunar disk sufficiently massive to later form the Moon (Canup and Asphaug 2001). Simulations of this *canonical case* consistently show that only about 20% of the mass of the (later) Moon is derived from the proto-Earth. Thus, it is surprising that lunar rocks show a strong elemental and isotopic similarity to the Earth's mantle, considering the elemental and isotopic heterogeneity of different solar system materials. Equilibration of a partially molten and partially vaporized post-impact disk with a terrestrial rock vapour atmosphere has been put forward (Pahlevan and Stevenson 2007) to explain this similarity. However, so far no complete, quantitative model of this equilibration exists (Pahlevan et al. 2011). Here we present simulations of a new class of collisions with higher impact velocities and a steeper impact angle. They result in an iron-poor Moon with the angular momentum of the Earth-Moon system and a considerably higher fraction ($50 - 80\%$) of proto-Earth material in the moon-forming disk. Shock heating during impact is much stronger than in the canonical case and the proto-lunar disk material is initially vaporized to a larger extent, possibly facilitating additional re-equilibration of the post-impact disk with the terrestrial mantle. We also investigate the influence of impactor composition (in silicon, iron and ice) on the outcome of the collision.

The collisional parameters for the giant impact considered so far have been limited to low-velocity collisions at, or only slightly above mutual escape velocity between target and impactor. The Earth-Moon system did not loose more than 10% of its initial angular momentum ($1 L_{\text{E-M}}$) between the giant impact and today (Canup et al. 2001). In low-velocity collisions, very little mass and therefore also very little angular momentum is lost, compared to the total mass and angular momentum before the collision. Hence if impact velocity and angular momentum of the collision are fixed values, for a given impactor and target composition only one degree of freedom remains in the form of the product of the sine of impact angle and the impactor mass. Previous work therefore focussed on finding the optimum mass ratio between impactor and target. Most recent work suggests a mass ratio of 9:1 with a total mass of $1.05 M_\oplus$ (Canup 2004). Both the impactor

and the target are assumed to be differentiated bodies with a $30wt\%$ iron core and a $70wt\%$ silicate mantle. In all these low-velocity collisions the impactor loses kinetic energy whilst grazing past the target and is then dispersed into a disk around the target. As a result, the proto-lunar disk is composed mainly of impactor material. The fraction of target silicate to total silicate material in the disk

$$f_T = (M_{targ}/M_{tot})_{disk} \tag{5.1}$$

is only around 20% where M_{targ} and M_{tot} denote the silicate part of the part of the disk originating in the target and total disk mass. If we define a similar target silicate material fraction for the post-impact Earth, we can deduce a depletion factor

$$\delta f_T = \frac{(M_{targ}/M_{tot})_{\text{disk}}}{(M_{targ}/M_{tot})_{\text{post-impact Earth}}} - 1 \tag{5.2}$$

which directly reflects the compositional similarity between the proto-lunar disk and the silicate portion of the Earth. This is important because the disk does not have to be derived completely from terrestrial (or target) material to match observations. It suffices that the impactor contributes approximately the same fraction of material to the disk and the post-impact Earth. Therefore, it is this value δf_T that has to approach $\approx 0\%$ (within the respective errors) to match geochemical observations.

These geochemical observations indicate that the composition of lunar rocks is best understood if their source material is either derived mainly from the Earth's mantle, or if the lunar accretion disk was thoroughly re-equilibrated with Earth's mantle in the aftermath of the collision. The oxygen isotope compositions of the Earth and the Moon are so close to each other ($\Delta^{17}\text{O} \leq 5ppm$ (Wiechert et al. 2001)) that, e.g, for an impactor that is as different in ^{17}O as Mars (Δ17O 320 ppm), δf_T can be no larger than about $\approx 5\%$ (see Table 5.1 for the different values of δf_T required by the different isotopic systems and impactor compositions). However, as there are at least two chondrite groups (enstatite and CI chondrites) that plot on the terrestrial mass-dependent fraction line in the oxygen three isotope diagram (Clayton 1993), it is possible that the terrestrial composition is representative of a larger solar system reservoir, from which also the impactor could have been derived. A further constraint is the Si isotopic composition of Earth and Moon, which are also identical within error, but distinct from all chondrite groups, Vesta and Mars (Fitoussi et al. 2009; Georg et al. 2007). This was proposed to be the result of Si partitioning into the Earth's iron core, a process that is inefficient on planets that have less than $\approx 15 - 20\%$ of Earth's mass (Wade and Wood 2005). Therefore, this distinct isotopic signature cannot have formed independently on the moon, or the impactor (unless the impactor was on the very heavy end of the mass range (Canup 2004), again linking the Moon to the terrestrial mantle.

The lunar and terrestrial Mg/Cr ratios are similar (≈ 100 and ≈ 87) but differ clearly from the chondritic value (≈ 36), which has also been explained by incorporation of Cr into Earth's core, a process that is inefficient on planets of the size of Mars (Jones and Palme 2000). In addition, the $^{53}Cr/^{52}Cr$ ratio is identical within error for Earth and Moon, although it varies with heliocentric distance (Shukolyukov and Lugmair 2000). Finally, Earth and Moon have a similar Hf/W-ratio and essentially identical ε^{182}W values (Touboul et al. 2007). While in giant impact simulations both bodies may end up with an identical ε^{182}W value, in no case simulated by Nimmo et al. (2010) were the observed Hf/W-ratios simultaneously matched. From all these observations, it was concluded (Nimmo et al. 2010; Pahlevan et al. 2011) that either the moon had to be derived predominantly from the Earth's mantle, or that the post-impact disk and the Earth's mantle must have re-equilibrated. So far, the first of these two possible solutions was incompatible with the results of hydrodynamical simulations. In the following paragraphs, we present a new series of simulations, where for the first time a significantly higher fraction of the lunar material is derived from the Earth's mantle.

The collisions presented here fall into the broad regime of slow hit-and-run collisions (Asphaug et al. 2006), which has never before been considered for the giant impact. Because of the higher impact velocities ($1.2 - 4v_{esc}$) in this type of collisions, substantial mass and angular momentum can be lost in the process. Therefore the initial angular momentum is less constrained and can be considerably higher than $1L_{\text{E-M}}$. In hit-and-run collisions most of the impactor escapes, so that the disk fraction is elevated in target-derived materials. Table 1 in the supplementary online material shows a selection of around 60 simulations of this type performed by us. The higher impact velocities of these collisions are also encouraged by current models of terrestrial planet formation (O'Brien et al. 2006).

We used a standard SPH code with self-gravity and the ANEOS equation of state (Thompson and Lauson 1972) for iron and water ice and M-ANEOS (Melosh 2007) for silicate. All simulations used a resolution of around 500'000 particles and were performed in a similar manner as in previous work (Benz et al. 1985; Canup and Asphaug 2001; Canup et al. 2001; Canup 2004).

A reference case (*cA08*) uses initial parameters and conditions comparable to those used in the canonical case (Canup 2004) and successfully reproduces an iron-depleted proto-lunar disk massive enough to form a Moon. For each of our simulations, the Moon mass is calculated using the disk mass and the specific angular momentum (Kokubo et al. 2000). We found collisions with an angle of $30 - 40°$ and 1.20–$1.30v_{esc}$ are also successful to put target material into orbit, when using differentiated impactors with chondritic Si/Fe composition ($30wt$%Fe, $70wt$%SiO_2) and masses between $0.15 - 0.20M_{\oplus}$. Some cases in this regime show an iron excess of $> 5wt$% in the proto-lunar disk and are rejected, as in previous work (Canup 2004). The best chondritic case matching all constraints is obtained using an impact angle of $35°$ and a velocity of $1.20v_{esc}$,

where 56% of the material in the silicate part of the disk originates from the target and δf_T reduces to -35% compared to -66% in the canonical reference case. Figure 5.4 shows four consecutive snapshots of such a high velocity collision.

The origin of the matter ending up in the proto-lunar disk is mainly defined by the geometry of the collision and is determined during the very early phase when the impactor is accelerating the target material. This can be seen in Figure 5.6 where the particles which later end up in the disk are highlighted in bright colour. In the canonical case, the impactor grazes around the target's mantle and is deformed. Due to the low impact velocity, material supposed to end up in orbit around the Earth must not be decelerated too strongly in order to retain enough energy to stay in orbit. In the canonical case, this is only the case for the parts of the impactor mantle most distant to the point of impact and some minor part of the target's mantle. But if impact velocity is increased from $1.00v_{esc}$ (*cA08*) to $1.30v_{esc}$ (*cC01*), parts from deeper within the target mantle receive the right amount of energy for orbit insertion. The outer regions of the target mantle receive too much energy and leave the system. This material removes mass and angular momentum from the system. While in case *cB04* only $\approx 10\%$ of the initial angular momentum is removed, $\approx 45\%$ are removed in case cC06 (see table 1 in SOM).

If the collision geometry predominantly determines the fraction of target material in the proto-lunar disk, altering the size of the impactor by density changes should also change the target material fraction in the disk. A denser impactor with the same mass delivers the same momentum, while reducing "spill-over" of impactor material as it can be seen in figure 5.6. High density, iron-rich impactors might be a product of composition changing hit-and-run collisions (Asphaug 2010). We investigated this scenario with $50wt\%$ and $70wt\%$ iron core fraction impactors. With a $0.2M_{\oplus}$ impactor at 30° impact angle and $1.30v_{esc}$ impact velocity the target material fraction f_T increases from 57% (δf_T = -34%) in the chondritic case (*cC01*), to 64% (δf_T = -28%) in the $50wt\%$ iron core case (*fA01*) up to 75% (δf_T = -19%) in the $70wt\%$ iron core case (*fB06*). However with the target material fraction, also the bound angular momentum and iron content of the disk increase to unrealistic values. Apparently, reducing the "spill-over" also reduces the lost mass and therefore lost angular momentum.

We also looked into less dense but still fully differentiated impactors with a composition of $50wt\%$ ice, $35wt\%$ silicate and $15wt\%$ iron, typical for small bodies accreted in regions of the solar system beyond the snow-line. Such a volatile-rich impactor scenario with an oxidized mantle is motivated by terrestrial Pd-Ag and Cr, Sr isotope geochemistry data, suggesting the very late accretion of $10-20\%$ of CI-chondrite like material (Schönbächler et al. 2010). In this scenario, the efficiency of putting material into orbit is reduced compared to cases with denser impactors, though the fact that there is less impactor silicate material available to end up in the disk actually raises the target material fraction to 81%, and δf_T to -10% in the case of an $0.2M_{\oplus}$ impactor

hitting at $30°$ impact angle and $1.30 v_{esc}$ impact velocity. However the resulting silicate portion of the disk is not massive enough ($0.73\ M_{☾}$) to later form the Moon.

The target material depletions yielded by the different models are compatible with geochemical constraints, with the possible exception of oxygen (see table 5.1). They can also explain the difference in FeO content observed in the mantles of Earth and Moon (8wt% and 13wt% FeO, respectively[12]) by simple mixture of an impactor mantle with a certain FeO content and a proto-Earth with a FeO content of 8wt% (assuming this is the equilibrium value determined by the oxygen fugacity and core size (Righter et al. 2006)). A typical δf_T of -35% for a 0.2 ME impactor then results in an impactor mantle FeO content of 18%, identical with Mars (see Figure 1 in SOM).

While the high velocity collision scenarios suit the dynamical and geochemical post-impact constraints as required for Moon formation, they differ considerably from the canonical case in terms of thermal history. The higher impact velocity leads to stronger shocks and therefore to more intense impact heating. Figure 5.5 shows cuts through the post-impact Earth after $\approx 58h$ with colour-coded temperature. In the canonical case (Figure 5.5 , left plot), only a thin blanket of material raining back from the disk experienced strong heating, while most of the mantle is only moderately heated above the initial average temperature of $2000K$ used in the simulation. In the high velocity case the shock is stronger and heats a substantial part of the mantle to temperatures above $10'000K$. Beside possible implications for the early history of the Earth, this also constitutes a different starting point for the re-equilibration model (Pahlevan and Stevenson 2007), where the mantle of the post-impact Earth has to be fully convective in order to allow full isotopic re-equilibration with the post-impact disk. While in the canonical model the thin hot blanket may inhibit convection at early stages, the much thicker hot layer which extends deep into the mantle in our model probably simplifies exchange of material between the post-impact Earth and the hot silicate vapor atmosphere. Our results not only relax the required efficiency of re-equilibration by starting with a disk with a higher target material fraction, but the resulting thermodynamical state might actually create a more favorable starting point for re-equilibration.

Another key difference to the canonical model is the dynamical state of the proto-lunar disk. In both models, material is ejected on ballistic trajectories after impact and forms an arm structure. Angular momentum is transferred from the inner to the outer parts, thus circularizing the orbit of the outer parts of the arm while the inner arm re-impacts the Earth. In the high velocity cases, this arm structure persists for a smaller time compared to the canonical case, transferring less angular momentum and leaving the material on more eccentric orbits. The dynamical evolution of such an eccentric disk and the consequences for Moon formation have yet to be studied.

In summary, our new approach of a high velocity ($1.30 v_{esc}$) hit-and-run collision can explain the isotopic similarity of the Earth and the Moon for all isotope systems except possibly oxygen (see table 5.1). This is a clear improvement over the canonical models (Canup 2004), where

none of the known isotopic similarities could be explained. Oxygen only cannot be explained by our model if the impactor indeed was as different in oxygen isotopes as Mars. In that case, a re-equilibration model (Pahlevan and Stevenson 2007; Pahlevan et al. 2011) might explain the similarity. Our work then also constitutes a new, hotter starting point for this re-equlibration model.

M.M.M. Meier and R. Wieler provided an overview of the geochemical constraints and motivated new simulations of the giant impact in regimes not yet considered before. A. Reufer and W. Benz performed the necessary simulations and the analysis of the data. All authors discussed the results and implications and commented on the manuscript at all stages. The authors have no competing interests or other interests that might be perceived to influence the results and/or discussion reported in this article.

We thank Maria Schönbächler, Kaveh Pahlevan and Vera Fernandes for discussions and Jay Melosh for providing us with the M-ANEOS package. Andreas Reufer and Matthias M. M. Meier were both supported by the Swiss National Science Foundation. All calculations were performed on the ISIS2 cluster at University of Bern.

Isotope system	Maximum Moon[1]	Mars		Ordinary Chondrite (average)		CI-chondrite		References
		Value	> δf_T	Value	> δf_T	Value	> δf_T	
$\delta^{17}O$	0.016‰	0.32‰	-5.0%	~1‰	-1.6%	~0‰[2]	N/A	[7]
$\delta^{30}Si$	-0.34‰	-0.58‰	-59%	-0.59‰	-58%	-0.6‰	-57%	[10], [25]
$\varepsilon^{53}Cr$	~-0.1	~-0.22	-45%	~-0.48	-21%	~-0.43	-23%	[13]
$\varepsilon^{182}W$	~0.19	~0.1 to 3.2[3]	-100% to -5.9%	(~-2)[4]	-	(~-1.9)[4]	-	[14], [27]

[1] Value of the isotopic composition that the moon could have while still being compatible with observations (within 2σ).
[2] CI chondrites plot on the terrestrial fractionation line. Their $\delta^{17}O$ offset from this line is therefore ~0‰. See main text for a discussion of possible implications.
3 Mars shows a large variety of $\varepsilon^{182}W$ values. -100% is for $\varepsilon^{182}W = 0.19$, -5.9% for an impactor with $\varepsilon^{182}W = 3.2$.
[4] An $\varepsilon^{182}W$ value of ~-2 is expected only for undifferentiated chondrites, but not for a differentiated impactor as assumed here. If a lunar composition of $\varepsilon^{182}W = -0.01$ is assumed, a very constraining depletion of -0.5% would result for an undifferentiated chondritic impactor.

Table 5.1: The constraints set by different isotopic systems on the value of δf_T. Reading example: If the impactor has the same isotopic composition in ^{17}O as Mars ($+0.32‰$), the closest-to-impactor value the moon could have still compatible with observations (in this case: $+0.016‰$) constrains the maximum depletion of terrestrial material in the moon-forming disk to 5.0%. In other words, the disk got only up to 5.0% more material from the impactor than the Earth as a whole (identical to the value in (Wiechert et al. 2001)). It is obvious from this table that the O isotope measurements are the most constraining. For comparison, the canonical model (*cA08*) yields a δf_T of -66%, incompatible with all listed isotopic systems. Reference keys: [7] Wiechert et al. (2001), [10] Georg et al. (2007), [13] Shukolyukov and Lugmair (2000), [14] Touboul et al. (2007), [25] Fitoussi et al. (2010), [27] Kleine et al. (2009).

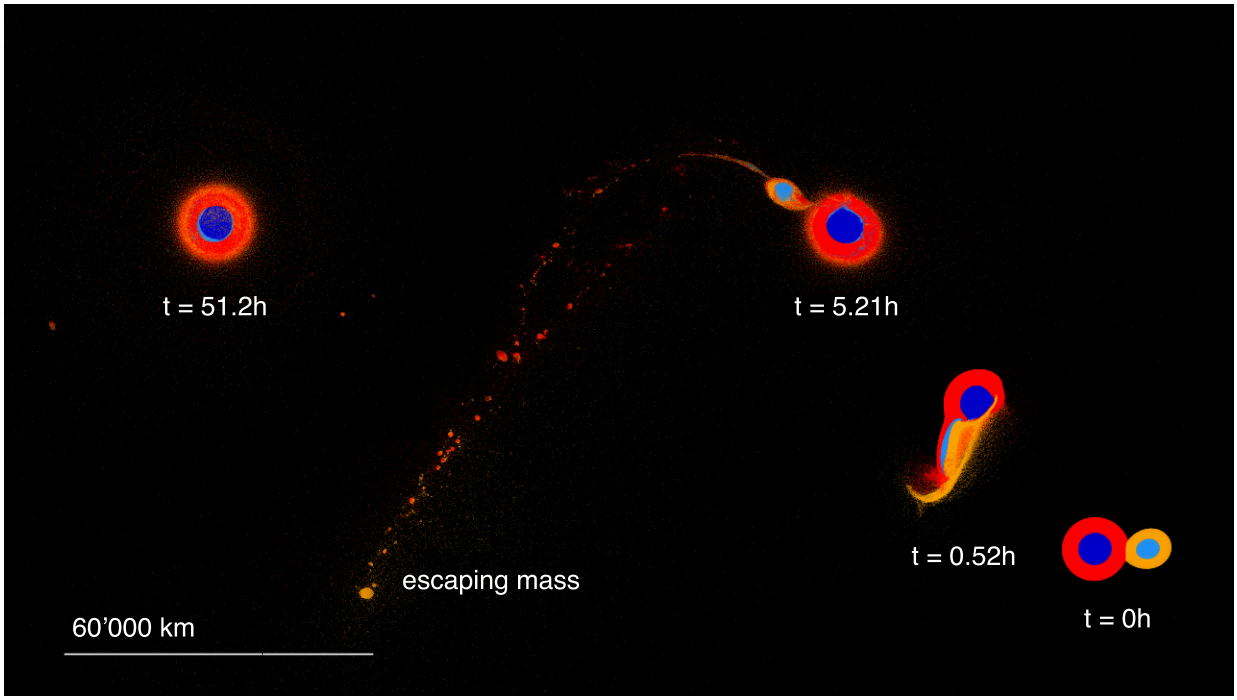

Figure 5.4: Four snapshots from the $30°$ impact angle and $1.30 v_{esc}$ impact velocity case (*cC06*) showing cuts through the impact plane. Colour coded is the type and origin of the material. Dark and light blue indicate target and impactor iron; Red and orange show corresponding silicate material. The far right shows the situation at the time of impact. At $0.52h$, it can be seen how the impactor ploughs deep through the targets mantle and pushes considerable amount of target material into orbit. A spiral arm of material forms and gravitationally collapses into fragments. The outer portions of the arm mainly consist of impactor silicates and escapes, while the fragments further inward enter eccentric orbits. The impactor iron looses angular momentum to the outer parts of the spiral arm and re-impacts the proto-Earth.

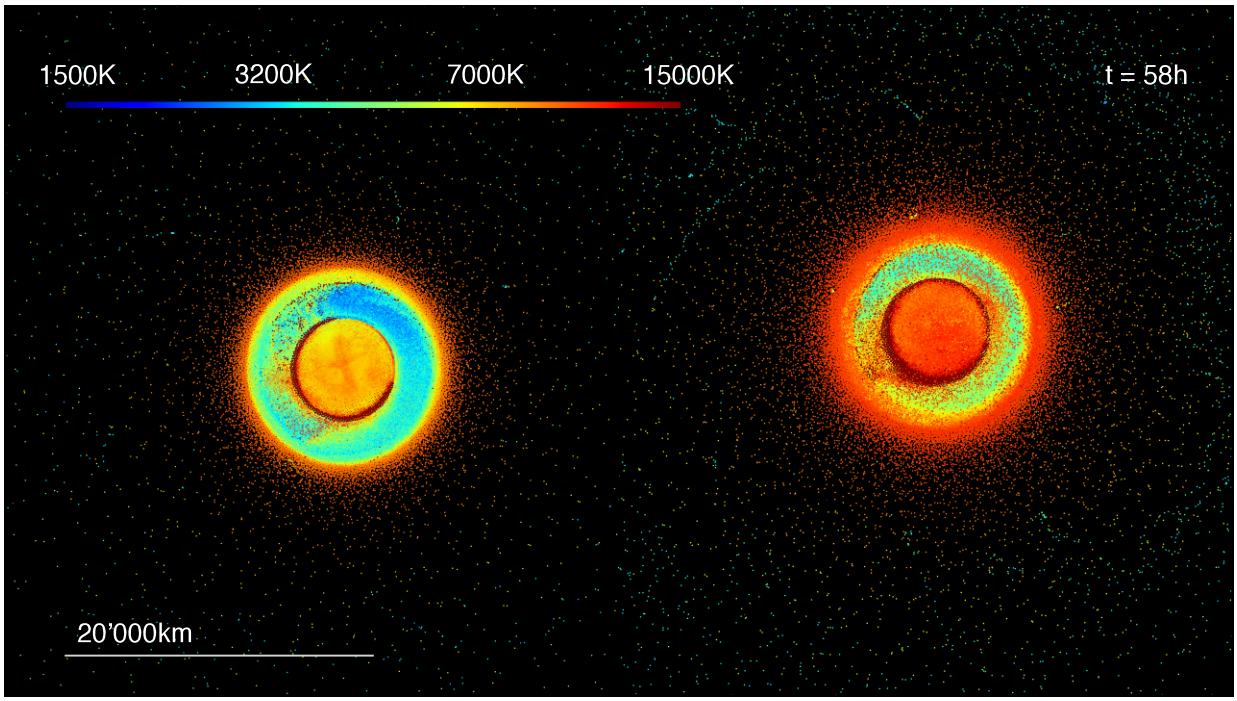

Figure 5.5: Comparing post-impact temperatures of the proto-Earth between the grazing reference simulation left (*cA08*) and the head-on case on the right (*cC06*). Colour coded is temperature in K in logged scale. The initial average temperature before the impact inside the target mantle is $\approx 2000K$.

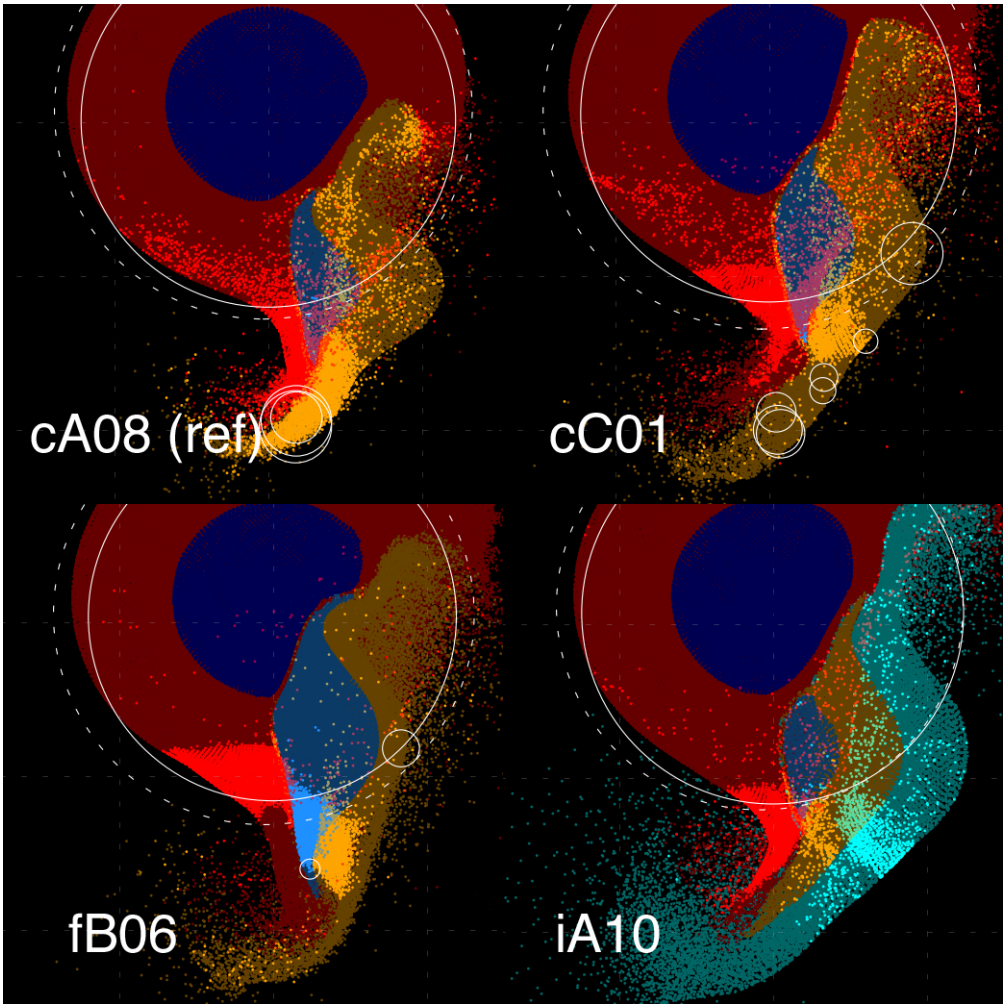

Figure 5.6: The origin of the disk material highlighted, half a collisional timescale ($(R_{imp} + R_{targ})/v_{imp}$) after impact. In the grazing reference case (*cA08*), the majority of the proto-lunar disk originates from a spill-over of the impactor. In the head-on cases (*cC01, fB06, iA10*), much more material comes from the target mantle, being pushed out into orbit by the impactor core. Colours are identical to figure 1. Turquoise on the right shows water ice for the icy impactor case *iA10*.

run	M_{tar} [M_E]	M_{imp} [M_E]	θ [°]	v_{imp} [v_{esc}]	impactor [wt% Fe/SiO_2/H_2O]	δf_T	f_T	M_{moon} [M_L]	L_D [L_{E-M}]	M_D [M_L] SiO_2	Fe	H_2O	L_{bound} [L_{E-M}]	L_{imp} [L_{E-M}]
cA01	0.90	0.10	30.0	1.35	30 / 70 / 0	-18%	77%	0.03	0.02	0.12	0.00	0.00	0.67	1.04
cA02	0.90	0.10	32.5	1.30		-26%	69%	0.05	0.02	0.13	0.01	0.00	0.70	1.07
cA03	0.90	0.10	32.5	1.50		-35%	61%	0.10	0.03	0.18	0.02	0.00	0.57	1.24
cA04	0.90	0.10	35.0	1.30		-36%	60%	0.16	0.05	0.23	0.06	0.00	0.68	1.14
cA05	0.90	0.10	35.0	1.35		-36%	61%	0.20	0.06	0.26	0.07	0.00	0.64	1.19
cA06	0.90	0.10	35.0	2.00		-31%	68%	0.02	0.01	0.09	0.01	0.00	0.33	1.76
cA07	0.90	0.10	45.0	1.00		-49%	46%	0.53	0.14	0.81	0.00	0.00	0.95	1.08
cA08	**0.90**	**0.10**	**48.0**	**1.00**		**-66%**	**31%**	**1.50**	**0.28**	**1.27**	**0.00**	**0.00**	**0.97**	**1.14**
cA09	0.90	0.10	50.0	1.00		-66%	32%	0.68	0.15	0.80	0.02	0.00	0.94	1.18
cA10	0.90	0.10	53.0	1.00		-75%	23%	0.89	0.21	0.96	0.15	0.00	0.96	1.23
cB01	0.90	0.15	32.5	1.15	30 / 70 / 0	-41%	53%	0.10	0.03	0.23	0.00	0.00	1.06	1.49
cB02	0.90	0.15	35.0	1.15		-35%	58%	0.23	0.06	0.37	0.01	0.00	1.10	1.59
cB03	0.90	0.15	35.0	1.20		-33%	60%	0.53	0.15	0.86	0.05	0.00	1.06	1.66
cB04	**0.90**	**0.15**	**40.0**	**1.10**		**-41%**	**53%**	**1.20**	**0.27**	**1.41**	**0.04**	**0.00**	**1.16**	**1.71**
cC01	0.90	0.20	30.0	1.30	30 / 70 / 0	-34%	57%	0.52	0.16	1.00	0.06	0.00	1.20	2.18
cC02	0.90	0.20	32.5	1.20		-30%	61%	0.90	0.27	1.63	0.03	0.00	1.40	2.16
cC03	**0.90**	**0.20**	**32.5**	**1.25**		**-37%**	**54%**	**1.01**	**0.27**	**1.51**	**0.06**	**0.00**	**1.27**	**2.25**
cC04	0.90	0.20	32.5	1.30		-32%	58%	1.12	0.27	1.39	0.14	0.00	1.30	2.34
cC05	0.90	0.20	35.0	1.15		-36%	54%	1.32	0.35	1.98	0.03	0.00	1.46	2.21
cC06	**0.90**	**0.20**	**35.0**	**1.20**		**-35%**	**56%**	**1.24**	**0.29**	**1.60**	**0.01**	**0.00**	**1.28**	**2.31**
cC07	0.90	0.20	45.0	1.00		-54%	39%	1.30	0.31	1.61	0.06	0.00	1.74	2.37
cC08	0.90	0.20	50.0	1.00		-76%	20%	3.16	0.65	2.84	0.37	0.00	2.02	2.57
fA01	0.90	0.20	30.0	1.30	50 / 50 / 0	-28%	64%	0.95	0.29	1.50	0.37	0.00	1.40	2.16
fA02	0.90	0.20	35.0	1.20		-28%	63%	1.18	0.26	1.20	0.13	0.00	1.55	2.28
fA03	0.90	0.20	32.5	1.25		-31%	62%	1.16	0.29	1.41	0.25	0.00	1.48	2.23
fA04	0.90	0.20	35.0	1.25		-24%	67%	1.33	0.29	1.22	0.26	0.00	1.57	2.38
fA05	0.90	0.20	40.0	1.10		-33%	59%	1.17	0.29	1.56	0.09	0.00	1.68	2.34
fB01	0.90	0.10	30.0	1.35	70 / 30 / 0	-23%	74%	0.03	0.02	0.08	0.05	0.00	0.74	1.01
fB02	0.90	0.10	35.0	1.30		-28%	69%	0.38	0.11	0.37	0.30	0.00	0.78	1.12
fB03	0.90	0.10	40.0	1.10		-25%	73%	0.31	0.10	0.46	0.16	0.00	0.85	1.06
fB04	0.90	0.10	45.0	1.00		-19%	78%	0.39	0.11	0.59	0.12	0.00	0.89	1.06
fB05	0.90	0.10	48.0	1.00		-33%	64%	0.72	0.18	0.51	0.54	0.00	0.97	1.12
fB06	0.90	0.20	30.0	1.30		-19%	75%	1.48	0.37	1.40	0.68	0.00	1.47	2.13
fB07	0.90	0.20	30.0	1.35		-18%	76%	1.63	0.38	1.38	0.71	0.00	1.48	2.21

SOM Table 1.: Simulation results. Note that L_D and M_{moon} estimated according to (Kokubo 2000) considers all disk material, including any present iron and water ice. Successful simulations with matching satellite mass, iron depletion and bound angular momentum are printed in bold face.

run	M_{tar} [M_E]	M_{imp} [M_E]	θ [°]	v_{imp} [v_{esc}]	impactor [wt% Fe/SiO_2/H_2O]	δf_T	f_T	M_{moon} [M_L]	L_D [L_{E-M}]	M_D [M_L] SiO_2	Fe	H_2O	L_{bound} [L_{E-M}]	L_{imp} [L_{E-M}]
iA01	0.90	0.20	15.0	1.50		-6%	84%	-0.13	0.02	0.21	0.00	0.08	0.75	1.35
iA02	0.90	0.20	25.0	1.30		-26%	66%	0.17	0.09	0.47	0.00	0.19	1.12	1.92
iA03	0.90	0.20	25.0	1.35		-23%	69%	0.15	0.08	0.41	0.00	0.18	1.08	1.99
iA04	0.90	0.20	25.0	1.50		-16%	76%	0.07	0.07	0.47	0.00	0.16	0.92	2.21
iA05	0.90	0.20	25.0	1.75		-24%	71%	0.17	0.07	0.38	0.01	0.11	0.60	2.58
iA06	0.90	0.20	30.0	1.00		-20%	71%	0.20	0.10	0.20	0.00	0.52	1.28	1.74
iA07	0.90	0.20	30.0	1.15		-52%	43%	0.76	0.21	0.62	0.00	0.65	1.36	2.01
iA08	0.90	0.20	30.0	1.20		-62%	34%	0.91	0.23	0.75	0.00	0.59	1.35	2.09
iA09	0.90	0.20	30.0	1.25		-20%	72%	0.36	0.11	0.33	0.00	0.35	1.15	2.18
iA10	0.90	0.20	30.0	1.30		-10%	81%	0.60	0.17	0.73	0.00	0.33	1.12	2.27
iA11	0.90	0.20	30.0	1.32		-14%	78%	0.26	0.09	0.26	0.00	0.37	1.00	2.30
iA12	0.90	0.20	30.0	1.35		-10%	82%	0.32	0.11	0.45	0.00	0.30	0.96	2.36
iA13	0.90	0.20	32.5	1.25		-15%	77%	0.71	0.19	0.56	0.00	0.56	1.01	2.34
iA14	0.90	0.20	32.5	1.30	15 / 35 / 50	-23%	70%	1.08	0.23	0.79	0.00	0.36	1.09	2.44
iA15	0.90	0.20	32.5	1.35		-54%	42%	2.19	0.45	1.50	0.26	0.48	1.06	2.53
iA16	0.90	0.20	35.0	1.00		-60%	36%	1.35	0.32	0.70	0.00	1.03	1.51	2.00
iA17	0.90	0.20	35.0	1.10		-30%	63%	1.61	0.37	0.92	0.00	1.07	1.42	2.20
iA18	0.90	0.20	35.0	1.15		-60%	36%	3.03	0.59	1.50	0.00	1.23	1.57	2.30
iA19	0.90	0.20	35.0	1.20		-60%	36%	2.89	0.52	1.23	0.00	0.95	1.55	2.40
iA20	0.90	0.20	35.0	1.25		-56%	40%	2.26	0.50	1.73	0.16	0.74	1.23	2.50
iA21	0.90	0.20	35.0	1.30		3%	98%	-0.01	0.00	0.02	0.00	0.02	0.48	2.60
iA22	0.90	0.20	40.0	1.15		-70%	27%	8.14	1.39	2.80	0.80	1.97	2.03	2.58
iA23	0.90	0.20	45.0	1.00		-67%	30%	2.04	0.49	1.28	0.01	1.39	1.71	2.47
iA24	0.90	0.20	45.0	1.15		-61%	37%	0.09	0.04	0.09	0.00	0.19	1.14	2.84
iA25	0.90	0.20	45.0	1.20		-1%	97%	0.01	0.01	0.03	0.00	0.05	0.35	2.96
iA26	0.90	0.20	45.0	1.25		-10%	89%	0.01	0.01	0.03	0.00	0.04	0.35	3.08
iA27	0.90	0.20	60.0	1.00		-73%	24%	0.96	0.28	0.75	0.01	0.99	1.41	3.02
iA28	0.90	0.20	60.0	1.15		0%	100%	0.00	0.00	0.01	0.00	0.02	0.16	3.48

SOM Table 1. (continued)

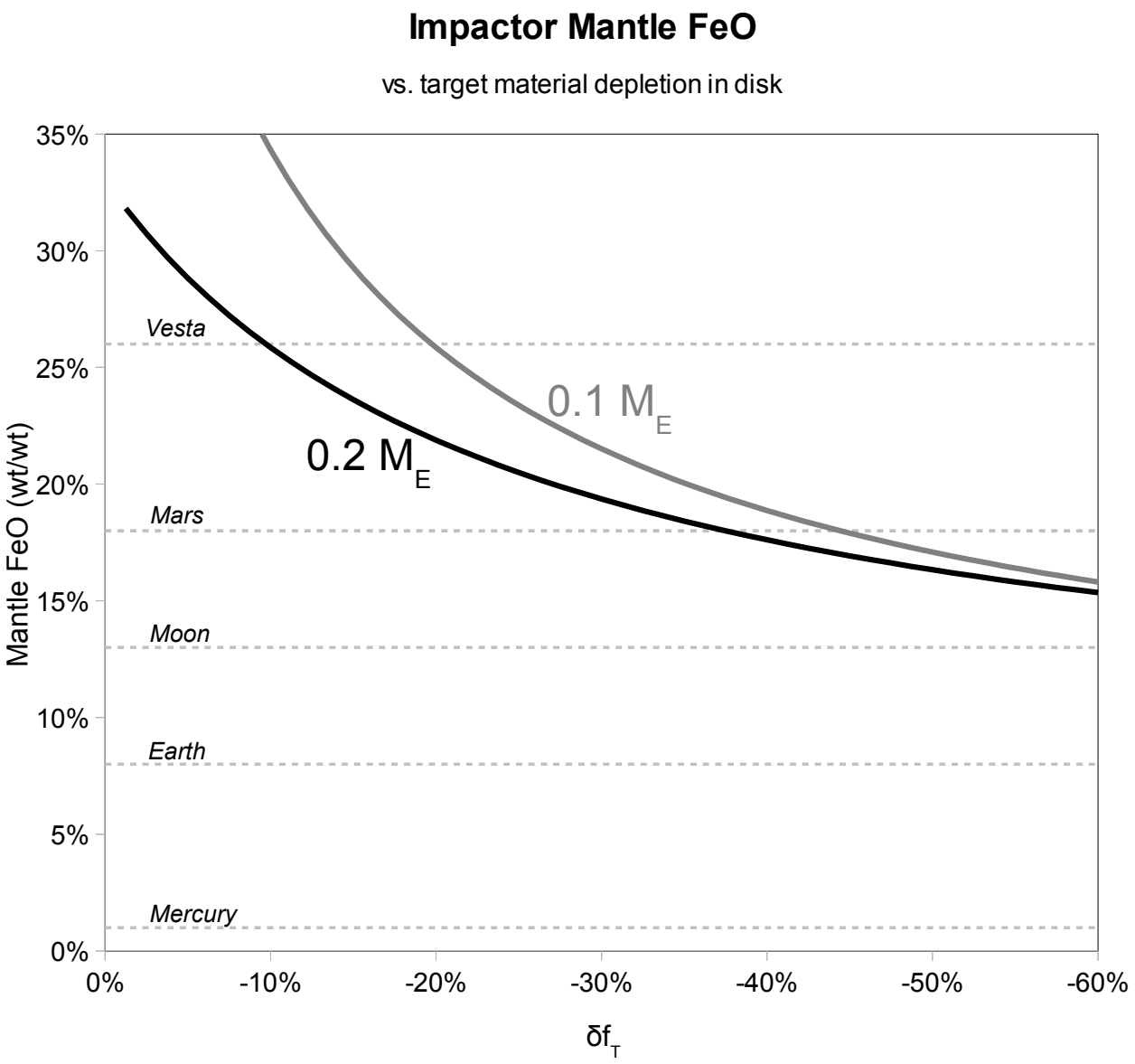

SOM Figure 1: The FeO content of the impactor's mantle (in wt%), if the Moon's content of 13wt% FeO is a mixture of Earth mantle (fixed at 8wt% FeO) and impactor mantle material, for an impactor of 0.2 (black line) and 0.1 (gray line) Earth masses. Note that an impactor with FeO = 18wt% (equal to Mars) yields a δf_T of -35% to -40%, a typical outcome of simulations as presented here. The mantle compositions of Mercury, Earth, Moon, Mars and Vesta are shown for comparison (Righter et al., 2006).

Bibliography

Erik Asphaug. Similar-sized collisions and the diversity of planets. *Chemie der Erde - Geochemistry*, 70:199, Jan 2010. doi: 10.1016/j.chemer.2010.01.004.

Erik Asphaug, Craig B Agnor, and Quentin Williams. Hit-and-run planetary collisions. *Nature*, 439:155, Jan 2006. doi: 10.1038/nature04311.

W Benz, W. L Slattery, and A. G. W Cameron. The origin of the moon and the single impact hypothesis ii. *Bulletin of the American Astronomical Society*, 17:726, Jun 1985.

W Benz, A. G. W Cameron, and H. J Melosh. The origin of the moon and the single impact hypothesis. iii. *Icarus (ISSN 0019-1035)*, 81:113, Sep 1989. doi: 10.1016/0019-1035(89)90129-2.

A. G. W. Cameron. The Origin of the Moon and the Single Impact Hypothesis V. *Icarus*, 126: 126--137, March 1997. doi: 10.1006/icar.1996.5642.

A. G. W Cameron. Higher-resolution simulations of the giant impact. *Origin of the earth and moon*, page 133, Jan 2000.

A. G. W. Cameron and W. R. Ward. The Origin of the Moon. In *Lunar and Planetary Institute Science Conference Abstracts*, volume 7 of *Lunar and Planetary Inst. Technical Report*, pages 120--+, March 1976.

R. M Canup and A. C Barr. Modeling moon-forming impacts; high-resolution sph and cth simulations. *41st Lunar and Planetary Science Conference*, 41:2488, Mar 2010.

Robin M Canup. Simulations of a late lunar-forming impact. *Icarus*, 168:433, Apr 2004. doi: 10.1016/j.icarus.2003.09.028.

Robin M Canup. Lunar-forming collisions with pre-impact rotation. *Icarus*, 196:518, Aug 2008. doi: 10.1016/j.icarus.2008.03.011.

Robin M Canup and Erik Asphaug. Origin of the moon in a giant impact near the end of the earth's formation. *Nature*, 412:708, Aug 2001.

Robin M Canup and Larry W Esposito. Accretion of the moon from an impact-generated disk. *Icarus*, 119:427, Feb 1996. doi: 10.1006/icar.1996.0028.

Robin M Canup, William R Ward, and A. G. W Cameron. A scaling relationship for satellite-forming impacts. *Icarus*, 150:288, Apr 2001. doi: 10.1006/icar.2000.6581.

J. E Chambers. Making More Terrestrial Planets. *Icarus*, 152:205, Aug 2001. doi: 10.1006/icar.2001.6639.

Robert N Clayton. Oxygen isotopes in meteorites. *In: Annual review of earth and planetary sciences. Vol. 21 (A94-10876 01-91)*, 21:115, Jan 1993. doi: 10.1146/annurev.ea.21.050193.000555.

C. Fitoussi, B. Bourdon, T. Kleine, F. Oberli, and B. C. Reynolds. Si isotope systematics of meteorites and terrestrial peridotites: implications for Mg/Si fractionation in the solar nebula and for Si in the Earth's core. *Earth and Planetary Science Letters*, 287:77--85, September 2009. doi: 10.1016/j.epsl.2009.07.038.

C. Fitoussi, B. Bourdon, K. Pahlevan, and R. Wieler. Si Isotope Constraints on the Moon-forming Impact. In *Lunar and Planetary Institute Science Conference Abstracts*, volume 41 of *Lunar and Planetary Inst. Technical Report*, pages 2653--+, March 2010.

R. B. Georg, A. N. Halliday, E. A. Schauble, and B. C. Reynolds. Silicon in the Earth's core. Nature, 447:1102--1106, June 2007. doi: 10.1038/nature05927.

W. K. Hartmann and D. R. Davis. Satellite-sized planetesimals and lunar origin. *Icarus*, 24:504--514, April 1975. doi: 10.1016/0019-1035(75)90070-6.

Shigeru Ida, Robin M Canup, and Glen R Stewart. Lunar accretion from an impact-generated disk. *Nature*, 389:353, Sep 1997. doi: 10.1038/38669.

J. H. Jones and H. Palme. *Geochemical Constraints on the Origin of the Earth and Moon*, pages 197--216. 2000.

T. Kleine, M. Touboul, B. Bourdon, F. Nimmo, K. Mezger, H. Palme, S. B. Jacobsen, Q.-Z. Yin, and A. N. Halliday. Hf-W chronology of the accretion and early evolution of asteroids and terrestrial planets. Geochim. Cosmochim. Acta, 73:5150--5188, September 2009.

Eiichiro Kokubo, Shigeru Ida, and Junichiro Makino. Evolution of a circumterrestrial disk and formation of a single moon. *Icarus*, 148:419, Dec 2000. doi: 10.1006/icar.2000.6496. (c) 2000: Academic Press.

H. J Melosh. A hydrocode equation of state for SiO_2. *Meteoritics & Planetary Science*, 42:2079, Jan 2007.

F. Nimmo, D. P. O'Brien, and T. Kleine. Tungsten isotopic evolution during late-stage accretion: Constraints on Earth-Moon equilibration. *Earth and Planetary Science Letters*, 292:363--370, April 2010. doi: 10.1016/j.epsl.2010.02.003.

D. P. O'Brien, A. Morbidelli, and H. F. Levison. Terrestrial planet formation with strong dynamical friction. *Icarus*, 184:39--58, September 2006. doi: 10.1016/j.icarus.2006.04.005.

K. Pahlevan, D. J. Stevenson, and J. M. Eiler. Chemical fractionation in the silicate vapor atmosphere of the Earth. *Earth and Planetary Science Letters*, 301:433--443, January 2011. doi: 10.1016/j.epsl.2010.10.036.

Kaveh Pahlevan and David J Stevenson. Equilibration in the aftermath of the lunar-forming giant impact. *Earth and Planetary Science Letters*, 262:438, Oct 2007. doi: 10.1016/j.epsl.2007.07.055.

K. Righter, M. J. Drake, and E. R. D. Scott. *Compositional Relationships Between Meteorites and Terrestrial Planets*, pages 803--828. Lauretta, D. S. & McSween, H. Y., 2006.

M. Schönbächler, R. W. Carlson, M. F. Horan, T. D. Mock, and E. H. Hauri. Heterogeneous Accretion and the Moderately Volatile Element Budget of Earth. *Science*, 328:884--, May 2010. doi: 10.1126/science.1186239.

A. Shukolyukov and G. W. Lugmair. On The 53Mn Heterogeneity In The Early Solar System. Space Sci. Rev., 92:225--236, April 2000.

D. J Stevenson. Origin of the moon - the collision hypothesis. *IN: Annual review of earth and planetary sciences. Volume 15 (A88-18742 06-91). Palo Alto*, 15:271, Jan 1987. doi: 10.1146/annurev.ea.15.050187.001415.

S.L. Thompson and H.S. Lauson. Improvements in the CHART D radiation --- hydrodynamic code III: revised analytic equations of state. *Technical Report*, SC-RR-71-0714, 1972.

M. Touboul, T. Kleine, B. Bourdon, H. Palme, and R. Wieler. Late formation and prolonged differentiation of the Moon inferred from W isotopes in lunar metals. Nature, 450:1206--1209, December 2007. doi: 10.1038/nature06428.

Keiichi Wada, Eiichiro Kokubo, and Junichiro Makino. High-resolution simulations of a moon-forming impact and postimpact evolution. *ApJ*, 638:1180, Feb 2006. doi: 10.1086/499032.

J. Wade and B. J. Wood. Core formation and the oxidation state of the Earth. *Earth and Planetary Science Letters*, 236:78--95, July 2005. doi: 10.1016/j.epsl.2005.05.017.

R. C. Weber, P.-Y. Lin, E. J. Garnero, Q. Williams, and P. Lognonné. Seismic Detection of the Lunar Core. *Science*, 331:309--, January 2011. doi: 10.1126/science.1199375.

U Wiechert, A. N Halliday, D.-C Lee, G. A Snyder, L. A Taylor, and D Rumble. Oxygen isotopes and the moon-forming giant impact. *Science*, 294:345, Oct 2001. doi: 10.1126/science.1063037.

J. Wolbeck and H. C. Connolly. Origin of the Moon: Icy Impactor Model (IIM). *Meteoritics and Planetary Science Supplement*, 73:5140--+, September 2010.